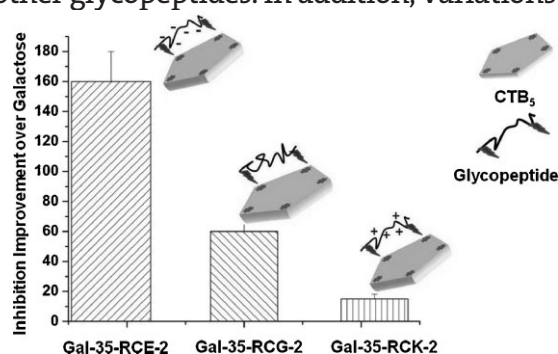


Manipulation of Electrostatic and Saccharide Linker Interactions in the Design of Efficient Glycopolyptide-Based Cholera Toxin Inhibitors^a

Ronak Maheshwari, Eric A. Levenson, Kristi L. Kiick*

Multivalent, glycopolymer inhibitors designed for the treatment of disease and pathogen infection have shown improvements in binding correlated with general changes in glycopolymer architecture and composition. We have previously demonstrated that control of glycopolyptide backbone extension and ligand spacing significantly impacts the inhibition of the cholera toxin B subunit pentamer (CT_{B5}) by these polymers. In the studies reported here, we elucidate the role of backbone charge and linker length in modulating the inhibition event. Peptides of the sequence AXPXG (where X is a positive, neutral or negative amino acid), equipped with the alkyne functionality of propargyl glycine, were designed and synthesized via solid-phase peptide synthetic methods and glycosylated via Cu(I)-catalyzed alkyne-azide cycloaddition reactions. The capacity of the glycopeptides to inhibit the binding of the B₅ subunit of cholera toxin was evaluated. These studies indicated that glycopeptides with a negatively charged backbone show improved inhibition of the binding event relative to the other glycopeptides. In addition, variations in the length of the linker between the peptide and the saccharide ligand also affected the inhibition of CT by the glycopeptides. Our findings suggest that, apart from appropriate saccharide spacing and polypeptide chain extension, saccharide linker conformation and the systematic placement of charges on the polypeptide backbone are also significant variables that can be tuned to improve the inhibitory potencies of glycopolyptide-based multivalent inhibitors.



R. Maheshwari, K. L. Kiick
Department of Materials Science and Engineering, University of Delaware, 201 DuPont Hall, Newark, Delaware 19716 USA
Fax: +1 (302) 831-4545; E-mail: kiick@udel.edu
E. A. Levenson
Department of Chemistry and Biochemistry, University of Delaware, Newark, Delaware 19716 USA
K. L. Kiick
Delaware Biotechnology Institute, 15 Innovation Way, Newark, Delaware 19711 USA

^a Supporting information for this article is available at the bottom of the article's abstract page, which can be accessed from the journal's homepage at <http://www.mbs-journal.de>, or from the author.

Introduction

Multivalent interactions play a pivotal role in biology and are present in numerous biomolecular interactions, such as those of glycoproteins, integrins, antibodies, and viruses.^[1] In particular, protein-carbohydrate interactions have been extensively investigated, since they play an important role in several processes, including pathogen recognition, inflammation, cell signaling, differentiation, and adhesion of various bacterial toxins.^[2,3] Given the relatively low affinity of the protein-carbohydrate interaction, nature

employs multivalent interactions between proteins and carbohydrates to increase the avidity of the interaction and provide specificity. This improvement in binding is often referred to as the “cluster glycoside effect”.^[4]

The dynamic nature of biological interactions suggests that a certain degree of flexibility may be valuable in designing multivalent constructs,^[5] to optimize both enthalpic and entropic effects during binding. In addition to the flexibility that appropriately designed multivalent polymer-ligand conjugates may offer, they also provide locally high concentrations of ligands, to yield greater binding avidity and specificity compared to their monovalent counterparts. The multivalent presentation of ligands also reduces the apparent disassociation rate of receptor-ligand complexes,^[6] which, in the long-term application of multivalent therapeutics, may afford advantages in efficacy and residence time.^[7] An additional advantage of multivalent approaches to ligand design is that polymer-based materials can be tailored to many varied architectures or conformations to optimize interactions with targets, via the utilization of appropriate polymeric scaffolds, monomeric ligands and conjugation strategies.^[8,9]

Significant research has been undertaken for the development of high affinity, polymer-derived multivalent ligands to inhibit multivalent interactions and selectively modify cell-signaling.^[1,10–24] In particular, these studies have focused on factors such as clustering of ligands, ligand density and valency, as well as length and interactions of intermolecular linkers. Many pioneering groups have contributed to this continually developing field.^[7,9,14,24–27] For instance, the Kiessling group has created multivalent neoglycopolymers to promote the proteolytic cleavage of α -selectin and thereby potentially modulate inflammatory responses. In addition, multivalent 2,4-dinitrophenyl (DNP) antigens produced via ring-opening metathesis polymerization (ROMP) permitted studies of the relationship between B cell receptor (BCR) clustering, localization, internalization and signal amplification. The extent of signaling, degree of BCR clustering and antibody production were dependent on antigen valency, while the BCR internalization was not.^[28] Other works by this group examined the influence of multivalent ligand epitope density on the clustering of Con A.^[10,29,30] Sampson and coworkers also used ROMP to produce peptide-modified polymers that have elucidated details of the interaction of sperm protein fertilin β with its egg receptor.^[31] In another study directed at design of dendrimeric multivalent ligands, Cloninger and coworkers investigated the binding of a series of mannose-functionalized PAMAM dendrimers (generations two through six) with monovalent and divalent derivatives of Con A and reported a statistical increment in binding with increase in the generation of dendrimers.^[18,32] They also incorporated mannose and

glucose at controlled ratios and densities on dendrimers and showed that the avidity of the multivalent interaction can be easily manipulated by tuning the density and ratio of monovalent ligands.^[7] The significance of ligand density in the inhibition of anthrax toxin by peptide-modified polymers was also illustrated by the Kane group; in these studies, poly(*N*-acryloyloxysuccinimide) of controlled molecular weights was modified at various densities with the peptide ligand (HTSTYWWLDGAP), and the polymeric multivalent ligands exhibited an optimal ligand density for toxin inhibition.^[33]

We have investigated both the role of architectural control of the polymer backbone, as well as ligand presentation, in the binding of the B₅ subunit of cholera toxin (CT) by linear glycopolyptide inhibitors.^[34–36] Cholera toxin is produced by the *Vibrio cholerae* bacterium and has an AB₅ architecture shared by the *Escherichia coli* heat labile enterotoxins. The pentameric B₅ structure binds specifically to the ganglioside GM1 (Gal- β 1-3GalNAc β 1-4(Neu5Ac α 2-3)Gal- β 1-Glc-ceramide) present on the surface of intestinal epithelial cells and gains entry into the cell via endocytosis, upon which the A subunit is cleaved and initiates the catalytic events that result in host dehydration and diarrhea.^[37] From the crystal structure of GM1-bound CT it is known that two terminal sugars of the GM1 pentasaccharide, galactose and sialic acid, are mainly responsible for the interaction. The binding sites between adjacent B subunits are approximately 35 Å apart.^[37] The known structure and biological functions of CT render it a useful system for unraveling the design rules in the production of multivalent inhibitors, as well as to provide additional and detailed insights into the general design of multivalent ligands.

In our previous studies,^[34–36,38] we demonstrated the production of well-defined, high molecular weight and monodisperse glycopolyptides via recombinant methods, to study the role of multivalent interactions in the inhibition of CT. With these recombinantly produced glycopolyptides, we investigated the role of architectural control over the polymer backbone as well as ligand presentation in the binding of the CT B₅. Results from these studies indicated that optimal spacing of the saccharide ligands at a distance of 35 Å was an important parameter in designing improved inhibitors of CT binding, and also demonstrated that the composition of the polypeptide chain influences binding separate from considerations of saccharide spacing. When a high percentage of glycine residues (approximately 45%) was included in sequences that adopt a random-coil secondary structure, the glycopolyptides adopted compact structures that hindered binding, whereas charged polyglutamic acid-based glycopolymers exhibited improved inhibition owing to a larger hydrodynamic volume and improved accessibility of saccharide groups.^[35] We postulated that the ionic charge

of the glutamic acid residues might also afford additional advantages in binding, particularly if these charges could be placed judiciously and selectively along the polymer backbone, as is possible only via recombinant methods.

The crystallographic details of CT B₅ reveal that the regions around and between adjacent GM1 binding sites of CT B₅ contain multiple positively charged amino acid residues (as shown in Figure S1).^[37] The incorporation of glutamic acid residues in the chain and particularly around the saccharide ligand site might therefore play a dual role in both extending the polymer chain and complementing the positive charges around the saccharide-binding site of the CT B₅, resulting in additional improvements in the interaction of glycopeptides and glycopolypeptides with the CT B₅ surface.

In this work, we report three random-coil-based bivalent glycopeptides designed to carry different charges in testing of this hypothesis. Peptides that are either negatively charged [35-RCE-2 (XG AEAPEEG AEAPEEG AEAPEEG AEAPEEG AEAEPXG)], positively charged [35-RCK-2 (XG AKAKPKG AKAKPKG AKAKPKG AKAKPKG AKAKPXG)], or neutral [35-RCG-2 (XGAGAGPSG AGAGPSG AGAGPSG AGAGPSG AGAGPXG)] were designed and synthesized via solid-phase synthetic methods. The single letter abbreviations denote the appropriate amino acids, while the position X is representative of the terminal alkyne-functionalized amino acid propargylglycine. Root mean square distances of ca. 32–40 Å between propargylglycines were calculated by assuming a freely jointed chain model and were corroborated by molecular dynamic simulations and random flight models. The alkyne functionality of propargylglycine allows the coupling of azido-functionalized galactose with various length linkers via Cu-catalyzed azide alkyne [3 + 2] Huisgen cycloaddition.^[39] Three azido-functionalized galactopyranosides – azido-β-D-galactopyranoside, 2-azidoethyl-O-β-D-galactopyranoside, and 3-azidopropyl-O-β-D-galactopyranoside – were employed to modify the above peptides. Reverse-phase high performance liquid chromatography (RP-HPLC), electrospray ionization mass spectrometry (ESI-MS) and ¹H nuclear magnetic resonance (¹H NMR) spectroscopy confirmed the purity and quantitative modification of the peptides with the galactopyranosides. Gel permeation chromatography (GPC) and circular dichroic (CD) spectroscopy indicated the

hydrodynamic volume and secondary structures of the glycopeptides. A direct enzyme linked assay (DELA) was used to determine the glycopeptide-based inhibition of the binding of CT B₅, and illustrated the effect of charge and linker length on inhibition.

Experimental Part

Materials and Methods

Fmoc-protected natural amino acids, Fmoc-protected propargylglycine and 2-(¹H-benzotriazole-1-yl)-1,1,3,3-tetramethyluronium hexafluorophosphate (HBTU) were purchased from EMD Biosciences Inc. (San Diego, CA). The cholera toxin B₅ subunit horseradish peroxidase conjugate (CT B₅-HRP) was obtained from List Biological Laboratories (Campbell, CA). Ganglioside GD_{1b} and C96 Maxisorp microtiter plates were obtained from Matreya (Pleasant Gap, PA) and Fisher Scientific (Pittsburgh, PA) respectively. Azido β-D-galactopyranoside, 1,2,3,4,6-penta-O-acetyl-β-D-galactopyranoside, dimethylsulfoxide (DMSO), OH-[CH₂]₂-Br, OH-[CH₂]₃-Br, BF₃·Et₂O and all other reagents were obtained from Sigma-Aldrich Co. (St. Louis, MO) and were used as received without any further purification.

Peptide Synthesis

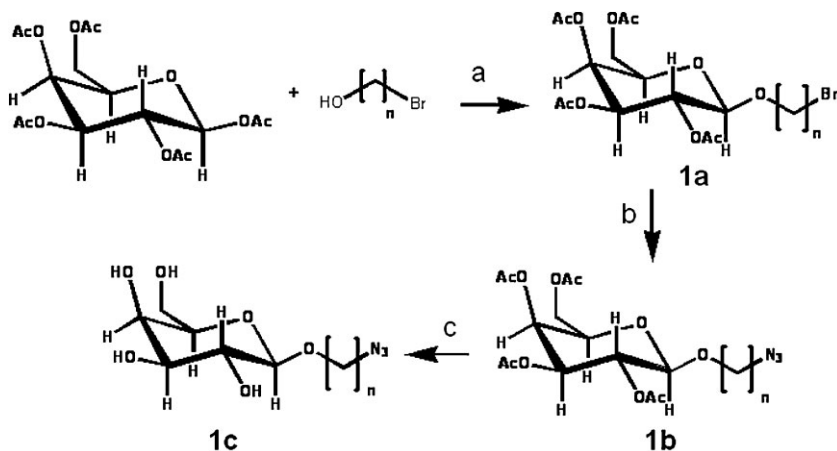
Peptides, with the sequences shown in Table 1, were synthesized via standard solid-phase peptide synthesis methods on a PS3™ automated peptide synthesizer (Protein Technologies, Inc., Tucson, AZ), using Rink amide MBHA resin as a polymer support. The amino acid residues were activated with HBTU in the presence of 0.4 M methyl morpholine in DMF. Deprotection reactions were carried out with 20% piperidine in DMF. Cleavage of the glycopeptides or peptide from the resin was performed in 95:2.5:2.5 trifluoroacetic acid (TFA)/triisopropylsilane (TIS)/water for 6–7 h. TFA was evaporated and cleavage products were precipitated in ether. The water-soluble glyco/peptides were dissolved in water and lyophilized. Peptides and glycopeptides were purified via reverse phase HPLC (RP-HPLC) (Waters, MA, USA), using a Symmetry C-18 column. Identities of peptides and glycopeptides were confirmed via ESI or MALDI mass spectroscopy and ¹H NMR spectroscopy.

Synthesis of Azido-Functionalized Galactopyranosides

Syntheses of azido-functionalized galactopyranosides as shown in Scheme 1 were conducted as previously reported.^[40] Three grams of

Table 1. Composition of synthesized peptides. X is propargylglycine.

Peptide	Sequence
35-RCE-1	GAEAEPEGAEAEPEGAEAEPEGAEAEPEGAEAEPEXGGGG
35-RCE-2	XGAEAEPEGAEAEPEGAEAEPEGAEAEPEGAEAEPEXGGGG
35-RCK-2	XGAKAKPKGAKAKPKGAKAKPKGAKAKPKGAKAKPXGGGG
35-RCG-2	XGAGAGPSGAGAGPSGAGAGPSGAGAGPSGAGAGPXGGGG

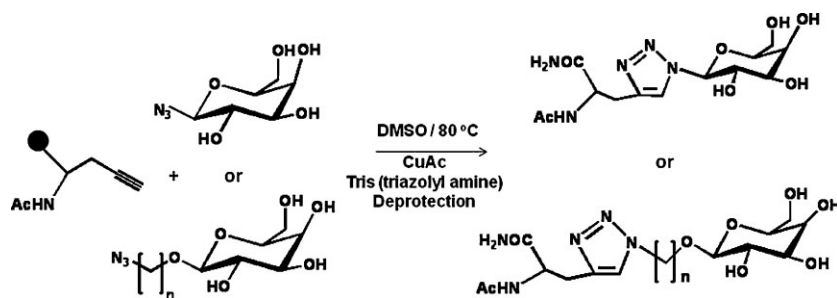


Scheme 1. Synthesis of azido-functionalized galactopyranosides with ethyl or propyl linkers; $n = 2$ or 3 , a: $\text{BF}_3 \cdot \text{OEt}_2$, CH_2Cl_2 , 0°C , b: NaN_3 , DMF, 100°C , and c: NaOMe in MeOH, Amberlite 15 resin.

1,2,3,4,6-penta-*O*-acetyl- β -D-galactopyranoside (7.7 mmol) and 1.5 eq of $\text{HO}-(\text{CH}_2)_n-\text{Br}$ were dissolved in dry DCM (25 mL) containing molecular sieves 4 \AA (1.5 g). The solution was cooled to 0°C and $\text{BF}_3 \cdot \text{Et}_2\text{O}$ (5 mL) was added slowly over a time period of 2 min. The reaction mixture was stirred overnight at 0°C and then diluted with excess DCM, followed by washing with a solution of cold water (200 mL), saturated NaHCO_3 (200 mL) and NaCl (200 mL) and drying using MgSO_4 . The solution was filtered and concentrated via rotary evaporation at 55°C . The identity of the product (**1a** in Scheme 1, light yellow syrup) was confirmed via ^1H NMR spectroscopy, ^{13}C NMR spectroscopy (CDCl_3) and ESI-MS (see the Supporting Information). **1a** and sodium azide (4 eq) were dissolved in DMF (15 mL) and stirred overnight at 100°C . Again the reaction mixture was diluted in DCM and unreacted sodium azide was removed by washing with excess cold water, saturated NaCl and drying using MgSO_4 . The solution was filtered and concentrated. De-acetylation of the azido-sugars (**1b**) was conducted by reaction with 5 eq of 25 wt.-% NaOMe/MeOH in dry methanol for 2 h. Sodium ions were exchanged with protons via treatment with Amberlite 15 resin. The final product (**1c**) was filtered and dried via rotary evaporation; evaluation of ^1H NMR and ESI-MS spectra (see the Supporting Information), coupled with comparisons to those previously reported,^[40] confirmed the identity and the essentially complete deacetylation of the saccharide products.

Synthesis of Tris(triazolyl amine)

Tripargyl amine (7.5 mmol) and benzyl azide (26.3 mmol) were dissolved in 10 mL of DMSO. Copper sulfate (0.378 mmol) and sodium ascorbate (1.89 mmol) were dissolved in 1 mL of water. The two solutions were mixed and stirred at 60°C for 12 h. The reaction product, tris(triazolyl amine), was purified via re-crystallization in CHCl_3 /ethyl ether.^[41] Theoretical and experimental $(\text{M} + \text{Na})^+ = 553.3 \text{ Da}$. The product was also characterized via ^1H NMR spectroscopy (see the Supporting Information), confirming its identity.^[41]



Scheme 2. General protocol for cycloaddition reactions performed on the solid phase.

Synthesis of Monovalent Saccharides and Monovalent/Bivalent Glycopeptides

For the synthesis of monovalent saccharide controls, Fmoc-propargylglycine was attached to Rink amide MBHA resin and the *N*-terminus of the amino acid was acetylated using acetic anhydride. The alkyne of the propargylglycine was then modified with azido- β -D-galactopyranoside, 2-azidoethyl-*O*- β -D-galactopyranoside or 3-azidopropyl-*O*- β -D-galactopyranoside via Huisgen 3 + 2 cycloaddition protocols, as shown in Scheme 2.^[41] Reactions were conducted on resin (solid phase) and the general protocol for the cycloaddition reaction was as follows: 1 eq of alkyne, 3 eq of azide, 0.5 eq of CuAc and 0.5 eq of tris(triazolyl amine) were dissolved in 2 mL DMSO, and the reaction was

carried out at 80°C for 24 h. Then the resin was thoroughly washed with thiourea, DMF and DCM to remove copper and other unreacted reactants. The glycosylated product was then cleaved from the resin as described above. For the synthesis of the monovalent and bivalent glycopeptides, the peptide sequences shown in Table 1 were first produced on the Rink amide MBHA resin, as described above. After synthesis of the peptide, the propargylglycine residues were glycosylated via the same procedure just described. All monovalent saccharides and all glycopeptides were purified using RP-HPLC and identities were confirmed via ^1H NMR spectroscopy and ESI-MS (see the Supporting Information).

Instrumental Methods

NMR Spectroscopy

^1H NMR spectra were acquired on a Bruker DRX-400 NMR spectrometer under standard quantitative conditions at ambient temperature. Electrospray ionization (ESI) mass spectrometry on saccharides, peptides and glycopeptides were performed at the Mass Spectrometry Facility in the Department of Chemistry and Biochemistry at the University of Delaware.

Circular Dichroic Spectroscopy

Circular dichroic spectra were recorded on a JASCO 810 spectrophotometer (Jasco, Inc., Easton, MD) using a 1 mm path length quartz cuvette. Samples with concentrations of approximate 50×10^{-6} M were prepared using PBS buffer (10×10^{-3} M phosphate, 0.150 M NaCl, pH 7.3) and scans were recorded by subtracting the PBS background. 400 μ L of samples were loaded in the quartz cuvette and the data points for the wavelength-dependent CD spectra were recorded with a 1 nm bandwidth.

Gel Permeation Chromatography

Gel permeation chromatography (GPC) was carried out to determine the relative hydrodynamic volume of peptides and glycopeptides for comparison with a control PGA30 peptide [poly(glutamic acid) with a degree of polymerization of approximately 30]. Samples were dissolved at approximately $1 \text{ mg} \cdot \text{mL}^{-1}$ in phosphate-buffered saline (PBS, pH 7.3), and filtered through a 0.22 μ m filter. The samples were separated using a Waters Ultrahydrogel Linear column (7.8×300 mm) followed by a Ultrahydrogel 250 (7.8×300 mm) column. Detection was achieved via the use of a Waters 2996 Photodiode Array Detector and a Waters 2414 Refractive Index Detector.

CT GD1b Direct Enzyme-Linked Assay

The GD1b direct enzyme-linked assays (DELA) were carried out in a 96-well format as previously reported.^[35,42] Microtiter plates were incubated at 37 °C for 16 h with 100 μ L (2 μ g/mL) ganglioside GD1b dissolved per well in PBS (pH 7.4). Unattached ganglioside was removed by washing the wells three times with PBS. Additional binding sites on the plate surface were blocked by incubating the wells with 200 μ L of a 1% (w/v) bovine serum albumin (BSA)-PBS solution for 30 min at 37 °C and then washing them three times with 0.05% Tween 20-PBS. All the glycopeptide samples were prepared by serial dilution from their stock solutions. Samples consisted of 6 ng \cdot mL⁻¹ cholera toxin B subunit conjugated to horseradish peroxidase (CTB₅-HRP) incubated for 2 h in the presence of ligand at varying concentrations. 100 μ L of these samples were incubated in a well for 30 min at room temperature and unbound toxin was removed by washing three times with 0.05% Tween 20-PBS. Toxin bound to GD1b was then revealed by addition of 100 μ L of Ultra TMB solution (Pierce) for 10–15 min followed by 100 μ L of 2 M H₂SO₄ and recording of the absorbance at 450 nm on a microtiter plate reader. IC₅₀ values were calculated from at least 10 different concentrations of saccharide ligands via non-linear regression analysis, as described previously,^[5] using the Microcal Origin software package.

Results

Synthesis of Glycopeptides

A series of well-defined, low molecular weight glycopeptides of random-coil secondary structure and different electrostatic charge were synthesized. These peptides were glycosylated with galactopyranosides with various linkers in order to evaluate the effects of electrostatic interactions

and linker arm on the CT B₅-inhibitory potency of the low valency and low molecular weight glycopeptides; these studies were intended to elucidate the salient features to be incorporated into recombinantly derived glycopolypeptides. The synthesized peptides (Table 1) with alkyne functionality from propargylglycine residues were modified with azido-functionalized galactopyranosides via Cu(I) alkyne-azide cycloaddition reactions.^[39] The glycosylation of the peptides (with protected amino acid side-chains) was carried out on the solid phase by using one of the three azido-functionalized galactopyranosides: azido- β -D-galactopyranoside, 2-azidoethyl-*O*- β -D-galactopyranoside or 3-azidopropyl-*O*- β -D-galactopyranoside. Glycopeptides were then deprotected (i.e., deprotection of the protected amino acid side chains) and cleaved from the resin, and purified via HPLC and characterized using ESI-MS and ¹H NMR spectroscopy (see the Supporting Information). The ¹H NMR spectra confirmed the maintenance of the β -linkage of the saccharides. The degree of glycosylation was measured via ¹H NMR spectroscopy and MS analyses, and was indicated to be greater than 90% for all glycopeptides, as shown in Table 2.

Secondary Structures of Glycopeptides

Circular dichroic (CD) spectroscopy was conducted in order to evaluate the secondary structures of the peptides and glycopeptides. The mean residue ellipticity as a function of wavelength was recorded for peptide and glycopeptide solutions (50×10^{-6} M in PBS buffer at pH 7.3) at 25 °C. As indicated in Figure 1, the spectra for all samples shows a minima near 198 nm, confirming the random-coil secondary structure of all peptides and glycopeptides,^[43] and confirming, as expected, that the modification of peptides with saccharides, with the concomitant formation of the triazole ring, does not affect the secondary structure of the peptide backbone. As also illustrated in the spectrum, the region near 220 nm shows identical positive bands (maxima) for the glutamic acid-rich and lysine-rich peptides and glycopeptides, consistent with previous spectra for extended poly-L-(glutamic acid) or poly-L-lysine at pH 7,^[44] suggesting a similar extended, random-coil secondary structure of the charged glycopeptides. In contrast, the spectrum of glycine-rich peptides and glycopeptides showed the absence of any positive band in this region, suggesting that they form a more compact random-coil secondary structure as would be expected based on their high glycine content (approximately 50% for the peptides).

Gel Permeation Chromatography

In our previous studies, we demonstrated that the hydrodynamic volumes of glycopolypeptides play a vital

Table 2. DELA results of monovalent saccharides and glycopeptides.

Inhibitor	Degree of glycosylation	IC_{50} (saccharide concentration)	Improvement over galactose	Molecular weight
		$10^{-3} \times M$		
Galactose	NA	30–45	1	180
Gal-PG ^{a)}	NA	$2.8 \pm 0.1^d)$	15	359
Gal-35-RCE-1	100 ± 1	$0.4 \pm 0.03^e)$	100	3 876
Gal-35-RCE-2	100 ± 2	$0.25 \pm 0.02^e)$	160	4 176
Gal-35-RCG-2	95 ± 2	$0.66 \pm 0.05^e)$	60	3 287
Gal-35-RCK-2	95 ± 3	$2.6 \pm 0.2^e)$	15	4 163
Gal-Et-PG ^{b)}	NA	$4.0 \pm 0.1^d)$	10	403
Gal-Et-35-RCE-2	100 ± 1	0.88 ± 0.03	45	4 264
Gal-Et-35-RCK-2	94 ± 2	>3	NA	4 251
Gal-Prop-PG ^{c)}	NA	$5.0 \pm 0.2^d)$	8	417
Gal-Prop-35-RCE-2	100 ± 2	>1	NA	4 292
Gal-Prop-35-RCK-2	92 ± 2	>3	NA	4 279

^{a)}Gal-PG: propargylglycine modified with azido- β -D-galactopyranoside; ^{b)}Gal-Et-PG: propargylglycine modified with 2-azidoethyl- O - β -D-galactopyranoside; ^{c)}Gal-Prop-PG: propargylglycine modified with 3-azidopropyl- O - β -D-galactopyranoside; ^{d)} IC_{50} values of monovalent saccharide ligands are significantly different from one another (Student's t -test showed $p < 0.05$); ^{e)} IC_{50} values of monovalent and divalent glycopeptides are significantly different from one another ($p < 0.05$).

role in their inhibitory potencies toward CT B₅.^[35] Thus, the relative retention times (and hydrodynamic volumes) of the peptides and glycopeptides (35-RCG-2, Gal-35-RCG-2, 35-RCE-2, Gal-35-RCE-1, Gal-35-RCE-2, Gal-Et-35-RCE-2 and Gal-Prop-35-RCE-2) were evaluated via GPC to evaluate the effects of charge on the hydrodynamic volumes relative to the PGA30 [poly(glutamic acid) with a degree of polymerization of approximately 30] employed in our original studies; the resulting data are shown in Figure 2. The absorbance at 214 nm was monitored as a function of time

for solutions of peptides and glycopeptides ($1 \text{ mg} \cdot \text{mL}^{-1}$) in PBS at pH 7.3; the observed peak widths for the peptides/glycopeptides were consistent with those obtained for monodisperse poly(ethylene oxide) (PEO) standards. As shown in the figure, PGA30, with the greatest charge density, eluted at the earliest time (14.4 min) and is therefore indicated to have the largest hydrodynamic volume. The somewhat pronounced shoulder in this peak results from the presence of a lower molecular mass species in this polydisperse macromolecule as it is received from

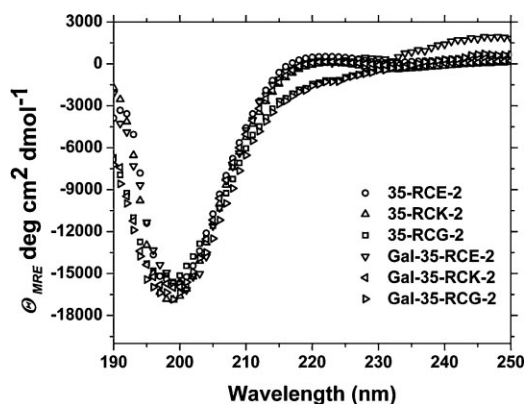


Figure 1. Circular dichroic spectroscopy results for peptides and glycosylated peptides (PBS, 25 °C).

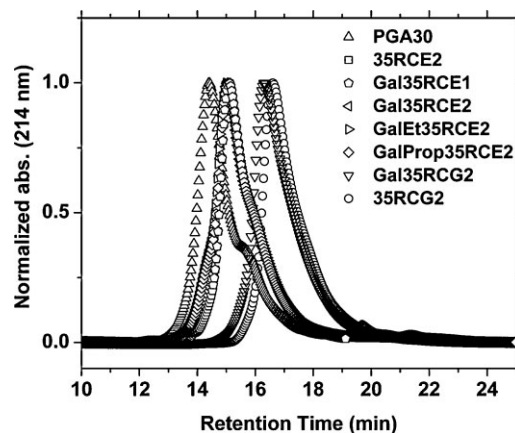


Figure 2. Gel permeation chromatography of peptides and glycopeptides compared to the standard peptide PGA30.

the manufacturer. The peptides 35-RCE-2 and 35-RCE-1 (and their corresponding glycopeptides), with approximately 35% glutamic acid content, exhibited mainly monomodal peaks with longer retention times (15.1 min for both peptides) and lower hydrodynamic volume compared to PGA30. A lower molecular mass shoulder is observed only for the Gal-RCE-1, and may result from the presence of a small amount of degradation products and/or unglycosylated species in this sample. The uncharged, glycine-rich 35-RCG-2 had the longest retention time of the peptides/glycopeptides (16.3–16.4 min), and the correspondingly lowest hydrodynamic volume, as expected. The high degree of glycine residues (approximately 50% for the peptide) and absence of any electrostatic repulsion causes 35-RCG-2 and Gal-35-RCG-2 to form a more compact conformation reflected in their higher retention times. The differences in the hydrodynamic volume of the peptides and their glycopeptides were negligible (the elution profiles for all 35-RCE-2 and 35-RCE-1-based peptides and glycopeptides overlapped), consistent with our previous results in which significant differences in the hydrodynamic volume of a polypeptide and its corresponding glycopolypeptide were only observed when there was a change in charge density due to glycosylation or methylation.^[35]

Inhibition Assays

The potential of these glycopeptides and monovalent saccharides to act as efficient inhibitors of the binding of CT B₅ was tested using competitive DELA experiments developed by Minke and coworkers.^[35,42] Inhibition curves from DELA experiments for different glycopeptides and monovalent saccharides as a function of saccharide concentration are shown in Figure 3 and 4. IC_{50} values

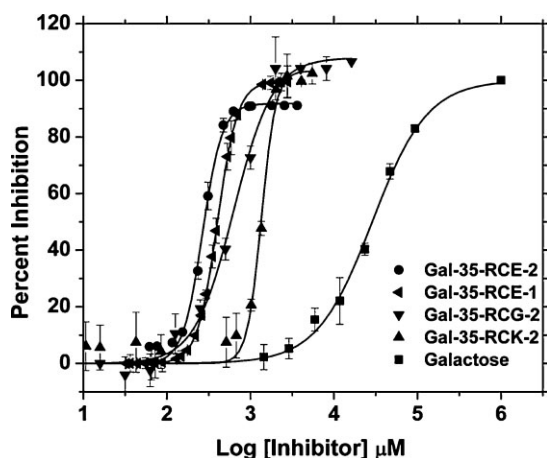


Figure 3. Dose response curves for the inhibition of CT B₅ binding by the glycopeptides (Gal-35-RCE-2, Gal-35-RCK-2, Gal-35-RCG-2 and Gal-35-RCE-1) and monovalent galactose as determined via DELA.

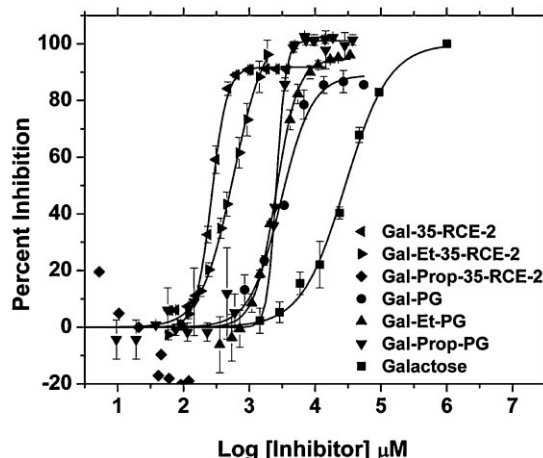


Figure 4. Dose response curves for the inhibition of CT B₅ by monovalent saccharides (Gal-PG, Gal-Et-PG and Gal-Prop-PG), glycopeptides (Gal-35-RCE-2, Gal-Et-35-RCE-2 and Gal-Prop-35-RCE-2) and galactose as determined via DELA.

for these various inhibitor species were calculated from the dose response inhibition curves and the inhibition improvements over monovalent galactose were compared, as shown in Table 2. Unmodified 35-RCE-Z ($Z = 1$ or 2) at concentrations greater than 1×10^{-3} M and 35-RCK-2 and 35-RCG-2 at concentrations greater than 1.5×10^{-3} M exhibited only a small degree of non-specific binding (less than 20%, not shown). There was no visible aggregation after addition of any inhibitors to the horseradish peroxidase (HRP)-linked CT B₅ (CT B₅-HRP). The concentrations of bifunctional glycopeptides were therefore varied from 0 to 3×10^{-3} M saccharide concentration (0 to 1.5×10^{-3} M peptide concentration) to minimize non-specific binding, while the concentration of the monovalent galactose was varied from 0 to 100×10^{-3} M.

Non-linear regression analysis of the dose response inhibition curves of glycopeptides yielded IC_{50} values (saccharide concentration) of 0.4×10^{-3} , 0.25×10^{-3} , 0.88×10^{-3} , 0.66×10^{-3} and 2.63×10^{-3} M for Gal-35-RCE-1, Gal-35-RCE-2, Gal-Et-35-RCE-2, Gal-35-RCG-2 and Gal-35-RCK-2, respectively. Galactose exhibits an IC_{50} of 40×10^{-3} M in these assays, consistent with previous reports.^[42,45] The improvements in inhibition for these glycopeptides compared to monovalent galactose were 100, 160, 45, 60 and 15, respectively. Gal-Prop-35-RCE-2 did not show any inhibition up to 1×10^{-3} M concentration and Gal-Et-35-RCK-2 and Gal-Prop-35-RCK-2 did not show any inhibition up to 3×10^{-3} M concentration (see the Supporting Information). IC_{50} values for these glycopeptides were therefore not evaluated, because nonspecific interactions from the peptide backbone might begin to interfere at these high concentration values. DELA experiments conducted on the three monovalent saccharides Gal-PG, Gal-Et-PG and

Gal-Prop-PG (at concentrations of 0 to 40×10^{-3} M) exhibited IC_{50} values of 2.8×10^{-3} , 4.0×10^{-3} and 5.0×10^{-3} M respectively, as shown in Figure 4 and Table 2, corresponding to 15-, 10- and 8-fold improvements over galactose. Although the differences in the slopes of these inhibition curves suggest that there may be slight variation in the mode of inhibition or that aggregation may be occurring, no aggregation was apparent in these samples or in previous samples analyzed via DLS.^[46]

Discussion

Design of Glycopeptides

In our previous studies, we reported that glycopolypeptides with large hydrodynamic volumes (V_h) arising from their high negative charge density, and with spacing between adjacent saccharide ligands similar to the CT binding sites, exhibit higher inhibitory potencies against CT relative to more flexible and more neutral glycopolypeptides.^[35] Our previous results showed that the larger V_h of glycopolypeptides, even for those glycopolypeptides of relatively low molecular weight, was correlated with improved toxin inhibition most likely due to the better accessibility of pendant saccharides. While the previous glycopolypeptides were negatively charged, similar chain extension might be possible via the use of positively charged amino acids, and variations in electrostatic interactions may render one type of chain an improved inhibitor. The solved crystal structure of the complex of CTB₅ and GM1 reveals that the regions between the GM1 binding sites of CTB₅ are composed of mainly positively charged (and neutral) amino acid residues as illustrated in Figure S1.^[37] The path between two adjacent binding sites, approximately 35 Å in length, is not severely hindered by any amino acid residue side-chains. The use of negatively charged glycopeptides, rather than positively charged chains, should likely enhance binding through additional electrostatic interactions with the basic, positively charged surface of CTB₅ around the saccharide binding pocket. Recombinant methods of glycopolypeptide design would allow the synthesis of such polypeptides in which the position of negatively charged amino acids can be specified.

Given our ultimate interests in the design of such glycopolypeptides, peptides of random-coil secondary structure, with the sequences shown in Table 1, were synthesized to compare the role of overall backbone charge on the inhibitory potencies of these molecules. The inclusion of high percentages of charged residues or glycines, with their different characteristic ratios (C_∞ for Gly-rich polypeptides of ≈ 2 –3.2 and C_∞ for Glu- or Lys-rich polypeptides of approximately 9),^[47] in the target glycopeptides permitted exploration of the inhibition differences

due to charge or peptide chain conformations.^[48] Since the negatively charged 35-RCE-Z ($Z=1$ or 2) and positively charged 35-RCK-2 peptide chains have similar characteristic ratios, they should exhibit similar conformational flexibility and hydrodynamic volumes (an extended random-coil secondary structure was suggested by the CD spectra),^[44,48] allowing assessment of the impact of backbone charge on the binding event. 35-RCG-2, a glycine-rich peptide in contrast, should exhibit a more flexible and compact conformation compared to the charged peptides 35-RCE-2 and 35-RCK-2. The root mean square (RMS) distances between the reactive propargylglycine residues (PG) in all three peptides were calculated assuming a freely jointed chain model with glycine as the point of joints. The RMS value in case of 35-RCG-2 was further confirmed by the random flight model using the formula $\langle R^2 \rangle = (C_n n_p l_p^2)$,^[47,49] where C_n is the characteristic ratio, n_p the number of segments, and l_p the length of each segment (here the distance between α -carbon atoms in the peptide bond, ca. 3.8 Å). Although C_n is dependent on the chain length, it is equal to C_∞ for poly(Gly) chains with $n > 10$,^[50,51] so C_n was assumed to be equal to C_∞ given that the peptides were 40 amino acids long; C_∞ was previously calculated to be 2–3.2 for glycine-rich peptides.^[47,49] The calculated average distance between PGs in 35-RCG-2 was 32–40 Å (by employing $C_n = 2$ –3.2). Similarly, calculated distances between PGs in 35-RCE-2 and 35-RCK-2 were within the range 35–42 Å, calculated assuming the freely jointed chain model and confirmed by molecular dynamic simulation studies in the case of the 35-RCE-2 (see the Supporting Information). Thus, the variation in charges in these peptide sequences should permit assessment of the differences in inhibition that arise due to differences in electrostatic interactions or peptide chain conformation.

The inclusion of alkyne-derivatized side-chains (via the use of propargylglycine) permits facile modification of the peptides with three different azido-functionalized galactopyranosides. These strategies are also useful for future studies of glycopolypeptide-based multivalent ligands, owing to the facile incorporation of the alkyne-functionalized homopropargylglycine in recombinantly derived proteins.^[52,53] The use of the three azido-functionalized galactopyranosides indicated in Scheme 2 results in linker arms of different lengths between the saccharide and peptide backbone, with corresponding differences in triazole positions with respect to the terminal galactose moiety. A comparison of the relative binding activity of the three monovalent saccharides therefore provides information about the interactions due to specific molecular contacts that could be made between the triazole ring and the CT B₅ binding site. Comparison of the inhibition by glycopeptides with the various saccharide ligands affords additional insight into the combined role of the linker and peptide backbone and their joint impact on inhibition.

Determining the Effects of Charge on the Inhibition of CT by Glycopeptides

Glycopeptides that were either negatively charged (Gal-35-RCE-Z), positively charged (Gal-35-RCK-2), or neutral (Gal-35-RCG-2) were tested as inhibitors of the cholera toxin B₅ subunit via the use of the competitive direct enzyme-linked assay (DELA) in which binding of CT B₅ to a GD1b-modified surface was monitored as a function of ligand concentration.^[35,42] The improvements in inhibition for these glycopeptides compared to monovalent galactose were 100, 160, 60 and 15 for Gal-35-RCE-1, Gal-35-RCE-2, Gal-35-RCG-2 and Gal-35-RCK-2, respectively. Given that the inter-residue spacing of the propargylglycines (and thus the saccharides) were indicated to be approximately the same for all peptides, the differences in inhibition improvement for the glycopeptides must arise due to the differences in either conformation and/or charge and suggest that negatively charged glycopeptides offer measurable advantages in inhibition. Although the differences in the actual free energy of binding are small for the glycopeptides, their statistically significant difference (see below) suggests the potential for electrostatic charge in altering the avidity of the binding event in glycopolypeptides of similar composition.

Role of Valency in the Inhibition of CT_{B5} by Negatively Charged Glycopeptides

The bivalent charged glycopeptides can interact with CT via interactions with the saccharide ligands, the linkers, and the charged backbone of the glycopeptide. Interactions of negatively charged monovalent (Gal-35-RCE-1) and divalent (Gal-35-RCE-2) glycopeptides with CT B₅ were compared to assess the differences in inhibition due to the valency of the saccharide unit. As shown in Table 2, there was a statistically significant difference ($p < 0.03$) in the inhibition of CT by Gal-35-RCE-1 (100-fold improvement over galactose) and Gal-35-RCE-2 (160-fold) over monovalent galactose. Given that the conformations (from CD) and hydrodynamic volumes (from GPC) of Gal-35-RCE-1 and Gal-35-RCE-2 were essentially identical, the differences in binding can be ascribed to the number of saccharides on the scaffold. The origins of the significant inhibition exhibited by the Gal-35-RCE-1 (100-fold improvement over galactose) likely arise from initial interaction of the saccharide with the CT B₅, strengthened by secondary interactions of the charged peptide backbone with the surrounding basic charged amino acid residues on the CT B₅. The importance of both the saccharide and peptide backbone interactions with CT B₅ in mediating this binding is suggested by the fact that the monovalent saccharide (Gal-PG) showed only a 15-fold improvement in binding over galactose, and by the additional fact the unmodified 35-RCE-Z peptides showed

no inhibition at these IC₅₀ concentrations, and hence nonspecific electrostatic interactions of the peptide backbone with the CT B₅ were not the primary origin of binding.

Role of Charge in the Inhibition of CT_{B5} by Glycopeptides

Glycopeptides Gal-35-RCE-2 and Gal-35-RCK-2 possess similarities in charge density (although opposite charge), side-groups, characteristic ratio,^[48] extended random-coil secondary structure (from CD spectroscopy studies) and hydrodynamic volumes. Thus, the saccharides in these two glycopeptides should have similar spacing and levels of accessibility for CT binding sites. However, Gal-35-RCK-2 exhibited only a 15-fold improvement in inhibition over monovalent galactose, as shown in Figure 5, demonstrating a significant difference in the inhibition potencies of these glycopeptides ($p = 0.002$). The regions proximal to the CT B₅ saccharide-binding sites contain basic amino acid residues (Figure S1), which may interact with the glycopeptide, and thus the presence of negative or positive charges on the glycopeptide might result in respective electrostatic attraction or repulsion with the CT B₅ surface upon saccharide binding. Consistent with this hypothesis, the data for Gal-RCE-2 and Gal-RCK-2, along with the data above for Gal-RCE-1, corroborate the role of the charge of the peptide in enhancing or diminishing the glycopeptide interactions with CT B₅. Toone and coworkers have also reported similar effects in the inhibition of Shiga-like toxin (SLT) by hydrophobic and hydrophilic bivalent glycopeptides (5 amino acids long) equipped with Pk trisaccharide ligands. Both the glycopeptides showed enhancements in inhibition over the monovalent Pk trisaccharide ligand and the extent of inhibition depended on the nature of the peptide. An approximately 20-fold enhancement in binding

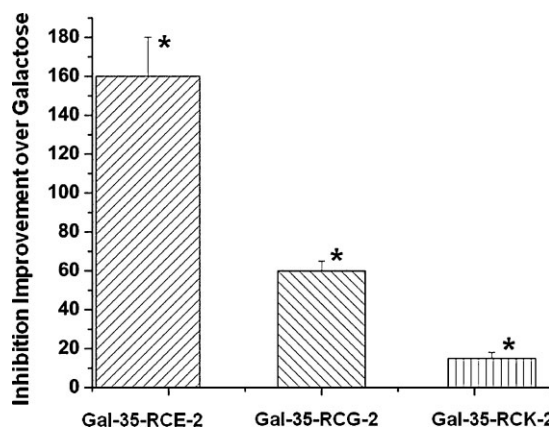


Figure 5. Comparison of the inhibition improvement values of glycopeptides Gal-35-RCE-2, Gal-35-RCG-2 and Gal-35-RCK-2 over galactose. * Indicates statistically significant differences in inhibition versus other scaffolds ($p < 0.05$).

was observed for glycopeptides with a hydrophobic spacer while only a 10-fold enhancement in binding was observed for glycopeptides with a hydrophilic spacer, as compared to the monovalent saccharide ligand.^[54]

The importance of the charge of the backbone was further underscored by comparisons of the inhibition improvements exhibited by Gal-RCE-2 (160-fold), Gal-RCK-2 (15-fold) and Gal-35-RCG-2, which exhibited a 60-fold improvement in inhibition relative to the monovalent galactose (Figure 5). The combination of CD spectroscopy and GPC studies showed that the compact glycine-rich glycopeptides exhibited a smaller hydrodynamic volume than the charged glycopeptides. In light of our previous studies that illustrated inhibition improvements with increasing hydrodynamic volumes, the Gal-RCE-2 glycopeptides may have been expected to show poorer inhibition than that of the charged glycopeptides of greater hydrodynamic volume, due to a combination of entropic and saccharide accessibility effects. The fact that the Gal-RCE-2 instead exhibited significantly improved inhibition ($p=0.005$) over that of the Gal-RCK-2 confirms the important role of charge in the inhibitory event. Thus, these studies suggest a key advantage in the use of glycopeptide and glycopolyptide approaches in the design of inhibitors: charged residues can be placed judiciously on the chain to affect inhibition via multiple mechanisms. The chain extension afforded by the inclusion of the glutamic acid residues may serve not only to improve saccharide accessibility, but also to reduce entropic penalties experienced by the chain upon binding, as the flexibility of the chain is reduced. In addition, complementary matching of the charges on the chain with the charges on the binding target also improves binding. The basic amino acid residues on CT B₅ in the region around the GM1 binding sites are present at approximately 10.6 and 14 Å when measured from the C_α of the basic residue to the C₄ of the terminal galactose of the GM1-bound ligand. In the sequence of Gal-35-RCE-2, glutamic acid residues adjacent to the saccharide are in the proximity of these distances, electrostatically complementing the basic charged amino acid residues of CT B₅, while the remaining glutamic acids provide chain extension. Such desired placement can also be expanded to polymeric polypeptide systems via recombinant methods.

Figure 6 shows the inhibition improvements for a range of glycopolyptide and glycopeptide inhibitors as a function of their retention time in the GPC experiment; these data illustrate the potential impact on inhibition of chain extension and matched architecture. The trend line in Figure 6 highlights the relationship of inhibition with retention time for heterogeneous glycopolyptides; it is clear from these data that the architecturally well-defined glycopolyptide Cap-35-RC-6 of our previous studies (Point B), with a saccharide spacing matched to that of

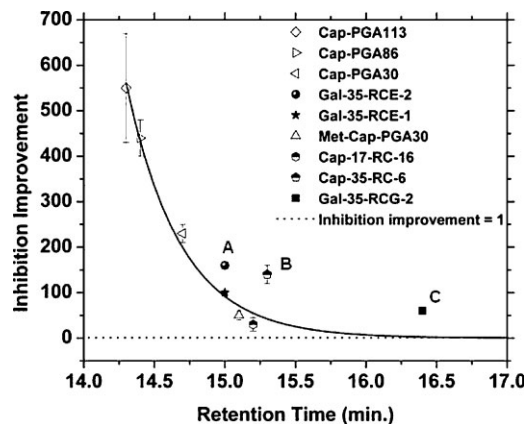


Figure 6. Comparison of the inhibitory potencies of glycopeptides and glycopolyptides^[35] as a function of retention time.

the CT B₅,^[35] exhibits inhibition that is improved over that expected on the basis of its size. The newly synthesized glycine-rich Gal-35-RCE-2 (Point A, the largest of the three species despite its low molecular mass), concomitant improvements in inhibition of CT B₅ were observed, again, with improvements greater than those expected on the basis of its size. This glycopeptides also shows inhibition greater than that of the other well-defined molecules. Thus, the inhibition exhibited by these glycopeptides and glycopolyptides supports that molecules with ligand spacing matched to the target receptors provide improvements in inhibition greater than those expected on the basis of hydrodynamic volume, and that increasing hydrodynamic volume with appropriate electrostatic complementarity provides further improvements in binding. These comparisons thus suggest that increasing the number of ligands by producing high molecular weight glycopolyptides with a similar sequence as that of 35-RCE-Z should result in inhibitors with much greater inhibitory potency.

Thus, despite previous reports that correlate mainly polymer molecular mass with inhibition potency,^[55–57] our study suggests that both variations in hydrodynamic volume (rather than molecular mass) and differences in charge can be exploited to enhance or diminish the inhibitory potencies of glycopeptide- and glycopolyptide-based inhibitors. Toone and coworkers had shown significant differences in the enhancement in inhibition of SLT by varying the hydrophobicity of glycopeptides (20- versus 10-fold).^[54] our findings demonstrate a much larger difference in the inhibition (160- versus 15-fold) of

CT B₅ by variations in the charge on the glycopeptide backbone. In addition, the improvements in inhibition exhibited by the glycopeptides here (up to 160-fold over galactose) are of the range usually observed for large and high valency linear glycopolymers and dendrimers.^[32,58–61] Although the inhibitory potencies by these glycopeptides are much smaller than the small pentavalent molecule inhibitors reported by Fan and coworkers,^[62] these designs allow assessment of the role of complementary secondary interactions in multivalent binding events. Hence these glycopeptide designs serve as the basis for designing new high molecular weight glycopolypeptide based inhibitors of higher binding avidity via appropriate choice of amino acid residues and architectural design.

Linker Architecture and Effect of Triazole Placement

Apart from polymer architectural features, the design of the linker which presents the saccharide or other ligand moieties is also important for designing inhibitors for bacterial toxins.^[63,64] GM1, a ganglioside found on the surface of intestinal epithelial cells, is the natural ligand for CT with a dissociation constant in the 10⁻⁹ M range.^[65] The majority of interactions in the CT-GM1 complex are from terminal saccharide moieties (from galactose with additional contributions from the sialic acid group) and thus maintenance of the terminal galactose as an anchor point for linkers of various compositions has been an approach previously adopted.^[66,67] For example, *m*-nitrophenyl α -galactoside (MNPG) was shown by Fan and coworkers to exhibit favorable interactions with the binding sites of CT B₅. In this saccharide ligand, the *m*-nitrophenyl group played a key role in the excellent inhibition observed, with X-ray crystallography studies on the complex of CT B₅-MNPG revealing that this saccharide ligand makes favorable contacts with the CT B₅ binding pocket via interactions of the nitro group with surrounding amino acids.^[68] In addition, *N*-(ϵ -aminocaproyl)- β -D-galactosylamine has been shown to elicit improvements in inhibition of CT B₅ through favorable hydrophobic interactions with the CT B₅ binding pocket.^[17,34,35] In this work, we employed alkyne-azide cycloaddition strategies, which result in the formation of a triazole group; this coupling strategy has been widely employed to modify polymers by attaching saccharide or other ligands.^[26,69] However, the impact on the binding event of the triazole and its placement has not yet been thoroughly probed in the design of multivalent systems. The large dipole and steric size of the 1,2,3-triazole, and the capacity of the N2 and N3 electron lone pairs to serve as hydrogen bonding acceptors,^[70] could affect the interaction of the triazole with the CT B₅ and alter binding. We thus maintained the terminal galactose and introduced the triazole group on a short hydrophobic chain; the

position of the triazole was varied to determine its impact on the inhibitory event.

Various monovalent saccharide linkers were made by modifying propargylglycine with azido-functionalized galactopyranosides [azido- β -D-galactopyranoside (Gal-PG), 2-azidoethyl-*O*- β -D-galactopyranoside (Gal-Et-PG), or 3-azidopropyl-*O*- β -D-galactopyranoside (Gal-Prop-PG)] via Cu(I)-catalyzed azide-alkyne cycloaddition (CuAAC),^[39,71] resulting in the formation of a triazole ring whose position, with respect to the galactose moiety, was varied by adjusting the length of the linker, as shown in Figure 7, which illustrates the lowest energy conformations of the three saccharide linkers determined at a temperature of 300 K by energy minimization calculations utilizing MM2 force fields.^[72,73] DELA evaluation of these three monovalent saccharides showed quite small but statistically significant differences ($p < 0.002$) in inhibition, with inhibition improvements of 15-, 10- and 8-fold over galactose for Gal-PG, Gal-Et-PG and Gal-Prop-PG respectively. The binding improvements observed for the Gal-PG are similar to *N*-(ϵ -aminocaproyl)- β -D-galactosylamine (data not shown),^[42] illustrating that the inclusion of a linker arm containing a triazole ring does not significantly reduce binding relative to a saccharide with an alkyl linker (or relative to the unmodified saccharide), although the specific origins of the improvements afforded by the inclusion of the triazole are not clear in the absence of crystal structure data. Interestingly, although the increased length (ca. 16–17 Å between the Gal C4 and the α -carbon of the amino acid) and hydrophobicity of the alkyl linker arm of *N*-(ϵ -aminocaproyl)- β -D-galactosylamine has been shown to improve this molecule's inhibition of CT B₅ over that of galactose,^[42] in our studies here, the Gal-PG, with the shortest and least hydrophobic linker (ca. 7–8 Å), shows slightly improved binding over that exhibited by Gal-Et-PG (ca. 11 Å) and Gal-Prop-PG (ca. 8–9 Å, shorter owing to the nonlinear trajectory). The placement of the triazole ring near the terminal galactose moiety in the Gal-PG may slightly improve binding via direct interaction of the triazole with the CT B₅ binding pocket, as observed for the nitrophenyl group in MNPG (see above) in the studies by Fan and coworkers. These effects may also arise from the

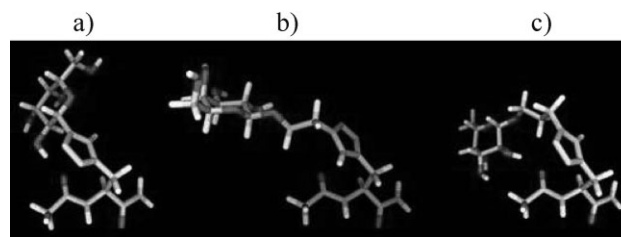


Figure 7. Lowest energy conformation of saccharide linkers: a) Gal-PG, b) Gal-Et-PG, and, c) Gal-Prop-PG.

impact of the triazole on the conformation of the linker arm (see below).

These three saccharides were conjugated to the glutamic acid-rich bivalent peptide 35-RCE-2. GPC results showed that there was essentially no variation in the hydrodynamic volumes, and CD spectra (data not shown) indicated no measurable differences in conformation, thus any differences in inhibition can be ascribed to differences in saccharide linker architecture. DELA experiments were performed on these three glycopeptides and the inhibition improvements over galactose were compared. Gal-35-RCE-2 and Gal-Et-35-RCE-2 exhibit IC_{50} values of 250×10^{-6} and 880×10^{-6} M (saccharide concentrations) which correspond to an inhibition improvement of 160- and 45-fold respectively over galactose ($p < 0.001$). Gal-Prop-35-RCE-2 did not show any inhibition up to 1×10^{-3} M peptide concentration, after which nonspecific interactions of the peptide backbone with the CT B₅ become apparent. The presentation of these three saccharides on the positively charged peptide backbone (35-RCK-2) showed a similar trend in the inhibition of CT binding. The Gal-35-RCK-2 exhibited the best inhibition of the three positively charged peptides, with the lowest IC_{50} value (2.63×10^{-3} M), as compared to Gal-Et-35-RCK-2 and Gal-Prop-35-RCK-2 with IC_{50} values of greater than 3×10^{-3} M ($p < 0.05$, SI). Given the marginal differences in inhibition by the monovalent saccharides, these results suggest that the disparity in the inhibition of CT B₅ by the glycopeptides may be due to differences in the accessibility of the saccharides on the different linkers when those linkers are anchored to the peptide chain. The charge of the chain further exacerbates these differences.

The lengths of linkers used in this study result in the formation of a triazole ring at different locations, resulting in a different conformation for each of the linkers (Figure 7). The most drastic deviation from a linear trajectory for the linkers occurred for the 3-azidopropyl-*O*- β -D-galactopyranoside derivative as shown in Figure 7c; there was also some evidence of a preferred nonlinear chain trajectory for the 2-azidoethyl-*O*- β -D-galactopyranoside derivative (Figure 7b). This increased length and preference for a nonlinear chain trajectory corresponds with slightly decreased inhibitory potencies for the monovalent triazole-linked saccharides that were substantially magnified when these saccharides were presented on a bivalent glycopeptide scaffold. In the simplest interpretation, the introduction of a kink in the linker arm with increasing linker length (when the saccharide is attached to the peptide) may force the galactose to lie closer to the peptide backbone resulting in a loss of accessibility and specificity for galactose in its interactions with CT. The accessibility of galactose in the case of Gal-Prop-PG is the worst due to the maximum deviation from a linear trajectory and consequently the inhibition of CT

by Gal-Prop-35-RCE-2 is even poorer than that of the monovalent Gal-Prop-PG. Any potential differences in conformational entropy loss of the peptide backbone for the three triazole-linked glycopeptides would further complicate these comparisons of inhibition; isothermal titration calorimetry experiments, as well as crystallography characterization, would shed more detail on these speculations. Nevertheless, it is clear from these studies that the position of the triazole ring, with its impact on the presentation of saccharide ligands attached to the peptide backbone, is an important variable in the design of related glycopolyptide-based inhibitors of CT B₅. Taken with the results above, our studies therefore suggest the high inhibitory potential of negatively charged, recombinantly produced polypeptide backbones, equipped with alkyne groups and modified via CuAAC protocols with Gal-PG-based saccharides. Production and characterization of such scaffolds is underway.

Conclusion

In this work, we have reported three bivalent glycopeptides with random-coil secondary structures and different charge identities. The presence of negative or positive charges on the glycopeptide resulted in respective electrostatic attraction or repulsion with the CT B₅ surface near the binding pocket, which significantly affected the inhibition exhibited by the glycopeptides. The negatively charged glycopeptides showed the greatest inhibition and the positively charged glycopeptides showed the worst inhibition; a neutral glycine-rich glycopeptide showed intermediate inhibition despite its smaller size and lower saccharide accessibility, underscoring the role that charge plays in modulating the binding of polypeptide-based inhibitors to the CT B₅ target, and suggesting opportunities to specifically design those interactions in polymeric inhibitors produced via recombinant methods. In addition, the coupling of azido-functionalized galactose with various length linkers via Cu(I)-catalyzed azide-alkyne cycloaddition has also been shown to be useful in the generation of efficient inhibitors. The position of the triazole ring can be easily varied by adjusting the length of the linker, and our results demonstrate that a saccharide ligand equipped with the triazole ring adjacent to the galactose moiety shows better inhibition as compared to other geometries, most likely due to both the placement of the triazole ring and corresponding better accessibility of the terminal galactose on the glycopeptide scaffold. Our results point to the optimal design features for the production of inhibitors of bacterial toxins, and suggest the now-available possibility of employing such stringent design control in the production of improved multivalent ligands.

Acknowledgements: This work was funded in part by grant numbers 1-P20-RR017716 and 1-P20-RR015588 (instrument facilities) from the *National Center for Research Resources (NCRR)*, a component of the *National Institutes of Health (NIH)*. Its contents are solely the responsibility of the authors and do not necessarily represent the official views of the *NCRR* or the *NIH*. This work was also funded in part by the *Center for Neutron Science* at the *University of Delaware* under award (*US Department of Commerce*) number 70NANB7H6178. *Senthil Kandasamy* and *Ronald Larson* (*University of Michigan*) are thanked for conducting molecular dynamics simulations.

Received: May 18, 2009; Revised: July 15, 2009; Published online: September 24, 2009; DOI: 10.1002/mabi.200900182

Keywords: glycopeptides; glycopolypeptides; multivalency; toxin inhibition

- [1] J. Huskens, *Curr. Opin. Chem. Biol.* **2006**, *10*, 537.
- [2] M. Mammen, S.-K. Chio, G. M. Whitesides, *Angew. Chem. Int. Ed.* **1998**, *37*, 2755.
- [3] A. Varki, *Glycobiology* **1993**, *3*, 97.
- [4] Y. C. Lee, R. T. Lee, *Acc. Chem. Res.* **1995**, *28*, 321.
- [5] W. P. Bowen, J. C. Jerman, *Trends Pharm. Sci.* **1995**, *16*, 413.
- [6] K. Nishikawa, S. Sawasdikosol, D. A. Fruman, J. Lai, Z. Songyang, S. J. Burakoff, M. B. Yaffe, L. C. Cantley, *Mol. Cell* **2000**, *6*, 969.
- [7] M. L. Wolfenden, M. J. Cloninger, *Bioconjugate Chem.* **2006**, *17*, 958.
- [8] K. L. Kiick, *Science* **2007**, *317*, 1182.
- [9] L. L. Kiessling, J. E. Gestwicki, L. E. Strong, *Angew. Chem. Int. Ed.* **2006**, *45*, 2348.
- [10] E. J. Gordon, W. J. Sanders, L. L. Kiessling, *Nature* **1998**, *392*, 30.
- [11] N. Nagahori, S.-I. Nishimura, *Biomacromolecules* **2001**, *2*, 22.
- [12] M. Mammen, G. Dahmann, G. M. Whitesides, *J. Med. Chem.* **1995**, *38*, 4179.
- [13] H. Kamitakahara, T. Suzuki, N. Nishigori, Y. Suzuki, O. Kanie, C.-H. Wong, *Angew. Chem. Int. Ed.* **1998**, *37*, 1524.
- [14] E. J. Baird, D. Holowka, G. W. Coates, B. Baird, *Biochemistry* **2003**, *42*, 12739.
- [15] H. Lis, N. Sharon, *Chem. Rev.* **1998**, *98*, 637.
- [16] P. I. Kitov, H. Shimizu, S. W. Homans, D. R. Bundle, *J. Am. Chem. Soc.* **2003**, *125*, 3284.
- [17] E. K. Fan, Z. S. Zhang, W. E. Minke, Z. Hou, C. Verlinde, W. G. J. Hol, *J. Am. Chem. Soc.* **2000**, *122*, 2663.
- [18] S. L. Mangold, J. R. Morgan, G. C. Strohmeier, G.A.M., M. J. Cloninger, *Org. Biomol. Chem.* **2005**, *3*, 2354.
- [19] T. K. Dam, S. Oscarson, R. Roy, S. K. Das, D. Page, F. Macaluso, C. F. Brewer, *J. Biol. Chem.* **2005**, *280*, 8640.
- [20] E. J. Gordon, L. E. Strong, L. L. Kiessling, *Bioorg. Med. Chem.* **1998**, *6*, 1293.
- [21] J. D. Reuter, A. Myc, M. M. Hayes, Z. Gan, R. Roy, R. Yin, L. T. Piehler, R. Esfand, D. A. Tomalia, J. R. J. Baker, *Bioconjugate Chem.* **1999**, *10*, 271.
- [22] E. K. Woller, M. J. Cloninger, *Org. Lett.* **2002**, *4*, 7.
- [23] E. K. Woller, E. D. Walter, J. R. Morgan, D. J. Singel, M. J. Cloninger, *J. Am. Chem. Soc.* **2003**, *125*, 8820.
- [24] T. K. Dam, C. F. Brewer, *Biochemistry* **2008**, *47*, 8470.
- [25] Y. Lee, N. S. Sampson, *Curr. Opin. Struct. Biol.* **2006**, *16*, 544.
- [26] V. Ladmiraal, G. Mantovani, G. J. Clarkson, S. Cauet, J. L. Irwin, D. M. Haddleton, *J. Am. Chem. Soc.* **2006**, *128*, 4823.
- [27] J. C. Lee, K. A. Parker, N. S. Sampson, *J. Am. Chem. Soc.* **2006**, *128*, 4578.
- [28] E. B. Puffer, J. K. Pontrello, J. J. Hollenbeck, J. A. Kink, L. L. Kiessling, *ACS Chem. Biol.* **2007**, *2*, 252.
- [29] C. W. Cairo, J. E. Gestwicki, M. Kanai, L. L. Kiessling, *J. Am. Chem. Soc.* **2002**, *124*, 1615.
- [30] P. Mowery, Z.-Q. Yang, E. J. Gordon, O. Dwir, A. G. Spencer, R. Alon, L. L. Kiessling, *Chem. Biol.* **2004**, *11*, 725.
- [31] K. A. Baessler, Y. Lee, K. S. Roberts, N. Facompre, N. S. Sampson, *Chem. Biol.* **2006**, *13*, 251.
- [32] S. L. Mangold, M. J. Cloninger, *Org. Biomol. Chem.* **2006**, *4*, 2458.
- [33] K. V. Gujrati, A. Joshi, A. Saraph, V. Poon, J. Mogridge, R. S. Kane, *Biomacromolecules* **2006**, *7*, 2082.
- [34] B. D. Polizzotti, K. L. Kiick, *Biomacromolecules* **2006**, *7*, 483.
- [35] B. D. Polizzotti, R. Maheshwari, J. Vinkenborg, K. L. Kiick, *Macromolecules* **2007**, *40*, 7103.
- [36] S. Liu, K. L. Kiick, *Macromolecules* **2008**, *41*, 764.
- [37] E. A. Merritt, S. Sarfaty, F. Vandenakker, C. Lhoir, J. A. Martial, W. G. J. Hol, *Protein Sci.* **1994**, *3*, 166.
- [38] Y. Wang, K. L. Kiick, *J. Am. Chem. Soc.* **2005**, *127*, 16392.
- [39] H. C. Kolb, M. G. Finn, K. B. Sharpless, *Angew. Chem. Int. Ed.* **2001**, *40*, 2004.
- [40] J. A. F. Joosten, V. Loimaranta, C. C. M. Appeldoorn, S. Haataja, F. A. ElMaate, R. M. J. Liskamp, J. Finne, R. J. Pieters, *J. Med. Chem.* **2004**, *47*, 6499.
- [41] Q. Wang, T. R. Chan, R. Hilgraf, V. V. Fokin, K. B. Sharpless, M. G. Finn, *J. Am. Chem. Soc.* **2003**, *125*, 3192.
- [42] W. E. Minke, C. Roach, W. G. J. Hol, C. L. M. J. Verlinde, *Biochemistry* **1999**, *38*, 5684.
- [43] V. P. Saxena, D. B. Wetlaufer, *Proc. Natl. Acad. Sci. USA* **1971**, *68*, 969.
- [44] M. L. Tiffany, S. Krimm, *Biopolymers* **1973**, *12*, 575.
- [45] I. Vrasidas, N. J. De Mol, R. M. J. Liskamp, R. J. Pieters, *Eur. J. Org. Chem.* **2001**, 4685.
- [46] B. K. Shoichet, *J. Med. Chem.* **2006**, *49*, 7274.
- [47] L. Mandelkern, W. L. Mattice, *Biochemistry* **1971**, *10*, 1934.
- [48] W. G. Miller, C. V. Goebel, *Biochemistry* **1968**, *7*, 3925.
- [49] W. Shen, J. A. Kornfield, D. A. Tirrell, *Soft Matter* **2007**, *3*, 99.
- [50] T. H. Evers, E. M. W. M. van Dongen, A. C. Faesen, E. W. Meijer, M. Merckx, *Biochemistry* **2006**, *45*, 13183.
- [51] P. R. Schimmel, P. J. Flory, *Proc. Natl. Acad. Sci. USA* **1967**, *58*, 52.
- [52] J. C. van Hest, K. L. Kiick, D. A. Tirrell, *J. Am. Chem. Soc.* **2000**, *122*, 1282.
- [53] K. L. Kiick, J. C. M. van Hest, D. A. Tirrell, *Angew. Chem. Int. Ed.* **2000**, *39*, 2148.
- [54] J. J. Lundquist, S. D. Debenham, E. J. Toone, *J. Org. Chem.* **2000**, *65*, 8245.
- [55] J. E. Gestwicki, C. W. Cairo, L. E. Strong, K. A. Oetjen, L. L. Kiessling, *J. Am. Chem. Soc.* **2002**, *124*, 14922.
- [56] K. Totani, T. Kubota, T. Kuroda, T. Murata, K. I. P. J. Hidari, T. Suzuki, Y. Suzuki, K. Kobayashi, H. Ashida, K. Yamamoto, T. Usui, *Glycobiology* **2003**, *13*, 315.

- [57] A. Spaltenstein, G. M. Whitesides, *J. Am. Chem. Soc.* **1991**, *113*, 686.
- [58] J. E. Gestwicki, L. E. Strong, L. L. Kiessling, *Chem. Biol.* **2000**, *7*, 583.
- [59] K. H. Schlick, R. A. Udelhoven, G. C. Strohmeyer, M. J. Cloninger, *Mol. Pharmaceutics* **2005**, *2*, 295.
- [60] C. C. M. Appeldoorn, J. A. F. Joosten, F. A. el Maate, U. Dobrindt, J. Hacker, R. M. J. Liskamp, A. S. Khan, R. J. Pieters, *Tetrahedron-Asymmetry* **2005**, *16*, 361.
- [61] S. Yamaguchi, Y. Nishida, K. Sasaki, M. Kambara, C. L. Kim, N. Ishiguro, T. Nagatsuka, H. Uzawa, M. Horiuchi, *Biochem. Biophys. Res. Commun.* **2006**, *349*, 485.
- [62] Z. S. Zhang, E. A. Merritt, M. Ahn, C. Roach, Z. Hou, C. Verlinde, W. G. J. Hol, E. Fan, *J. Am. Chem. Soc.* **2002**, *124*, 12991.
- [63] P. Rai, C. Padala, V. Poon, A. Saraph, S. Basha, S. Kate, K. Tao, J. Mogridge, R. S. Kane, *Nat. Biotechnol.* **2006**, *24*, 582.
- [64] D. Arosio, M. Fontanella, L. Baldini, L. Mauri, A. Bernardi, A. Casnati, F. Sansone, R. Ungaro, *J. Am. Chem. Soc.* **2005**, *127*, 3660.
- [65] J. A. Mertz, J. A. McCann, W. D. Picking, *Biochem. Biophys. Res. Commun.* **1996**, *226*, 140.
- [66] A. Bernardi, A. Checchia, P. Brocca, S. Sonnino, F. Zuccotto, *J. Am. Chem. Soc.* **1999**, *121*, 2032.
- [67] A. Bernardi, D. Arosio, L. Manzoni, D. Monti, H. Posteri, D. Potenza, S. Mari, J. Jimenez-Barbero, *Org. Biomol. Chem.* **2003**, *1*, 785.
- [68] D. D. Mitchell, J. C. Pickens, K. Korotkov, E. Fan, W. G. J. Hol, *Bioorg. Med. Chem.* **2004**, *12*, 907.
- [69] J. Geng, G. Mantovani, L. Tao, J. Nicolas, G. Chen, R. Wallis, D. A. Mitchell, B. R. G. Johnson, S. D. Evans, D. M. Haddleton, *J. Am. Chem. Soc.* **2007**, *129*, 15156.
- [70] A. Brik, J. Alexandratos, Y. C. Lin, J. H. Elder, A. J. Olson, A. Wlodawer, D. S. Goodsell, C. H. Wong, *ChemBioChem* **2005**, *6*, 1167.
- [71] B. H. M. Kuijpers, S. Groothuys, A. R. Keereweer, P. J. L. M. Quaedflieg, R. H. Blaauw, F. L. vanDelft, F. P. J. T. Rutjes, *Org. Lett.* **2004**, *6*, 3123.
- [72] N. L. Allinger, *J Am Chem Soc* **1977**, *99*, 8127.
- [73] "CS Chem 3D Ultra", in: *CambridgeSoft Corp*, Cambridge, MA 2001.